

Excited-State Dynamics of 8'-Apo- β -caroten-8'-al and 7',7'-Dicyano-7'-apo- β -carotene Studied by Femtosecond Time-Resolved Infrared Spectroscopy

Yoonsoo Pang, Matthew A. Prantil,[†] Aaron J. Van Tassel,[‡] Garth A. Jones, and Graham R. Fleming*

Department of Chemistry, University of California, Berkeley, and Physical Biosciences Division, Lawrence Berkeley National Laboratory, Berkeley, California 94720-1460

Received: June 18, 2009; Revised Manuscript Received: August 4, 2009

We present infrared transient absorption measurements of the substituted apocarotenoids 8'-apo- β -caroten-8'-al (**I**) and 7',7'-dicyano-7'-apo- β -carotene (**II**) in the S₁ excited states by one-photon excitation (1PE) and two-photon excitation (2PE). 1PE populates the higher S₂ state, which converts to the S₁ state via rapid internal conversion, and 2PE populates the S₁ state directly. The 1PE-prepared population returns to the ground state on a ~19 ps time scale in **I** and a ~2.0 ps time scale in **II**. Distinct vibrational spectra and dynamics are observed from the 2PE-prepared S₁ state for both **I** and **II**: the symmetric C=C stretching vibration around 1500 cm⁻¹ in the S₁ state is several-fold increased in strength over other C=C stretching modes compared to the 1PE case, and long-lived absorptions are observed even after all the excited-state populations have decayed. The lifetimes of the S₁ state prepared by 2PE are slightly shorter (~17 ps for **I** and ~1.7 ps for **II**) than the 1PE values. It is proposed that 1PE and 2PE lead to the population of different conformational minima of the S₁ potential surface. These two minima do not communicate on the time scale of the S₁ lifetime and have different relaxation channels on the ground-state surface.

Introduction

Carotenoids play many roles in nature, depending on the structure, properties, and integration into protein structures; in plants, they are important in photoprotection^{1,2} and light-harvesting,^{3–5} while in humans they act as antioxidants² and provide photoprotection in vision.^{6,7} 8'-Apo- β -caroten-8'-al (**I**) is a naturally occurring carotenoid most commonly found in citrus fruit skins. In humans, **I** is produced in vivo from enzymatic asymmetric cleavage of β -carotene and can be the starting material for retinal formation.⁸ 7',7'-Dicyano-7'-apo- β -carotene (**II**) is synthesized by direct Knovenagel condensation of **I** with malononitrile in methanol using pyridine as a catalyst.⁹

The molecular structures of β -carotene, **I**, and **II** are shown in Figure 1. Polarized apocarotenoids **I** and **II** contain an electron-withdrawing carbonyl or cyano group on one terminal of the polyene chain and possess C_s symmetry rather than the C_{2h} symmetry of β -carotene: the ground state (S₀) and first singlet excited state (S₁) both possess A' symmetry, while the second singlet excited state (S₂) has A'' symmetry. The electronic structure of **I** and **II** is analogous to that of carotenoids with higher symmetry such as β -carotene, where the S₀ and S₁ states possess A_g symmetry while S₂ is of B_u symmetry.^{10,11} The strong absorption band in the visible region of the spectrum for **I** and **II** is due to the S₀ → S₂ transition. The S₁ excited states of **I** and **II** cannot be populated by one-photon absorption from the ground state since this process is forbidden by symmetry. However, the S₀ → S₁ transition is allowed by two-photon excitation (2PE) of near-infrared light. The selection rules for electronic transitions in asymmetric carotenoids such

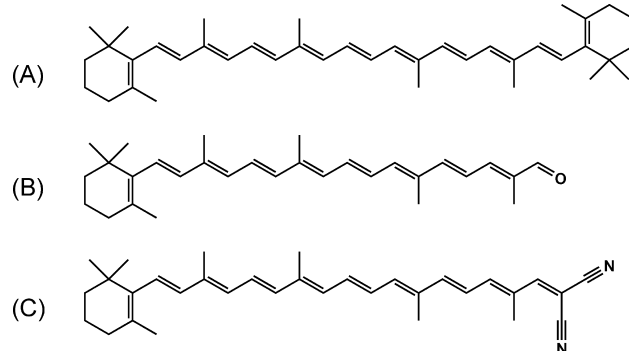


Figure 1. Structure of (A) β -carotene, (B) 8'-apo- β -caroten-8'-al (**I**), and (C) 7',7'-dicyano-7'-apo- β -carotene (**II**).

as **I** and **II** are similar to the case of carotenoids in the idealized C_{2h} point group since their properties are mainly determined by conjugated polyene chains.

The excited-state dynamics of **I** and **II** has been studied by several research groups as model systems for highly symmetric carotenoids and open-chain carotenoids such as spheroidene.^{12–17} Population of the S₂ state of **I** and **II** by one-photon excitation (1PE) from the ground state leads to ultrafast transfer via a putative conical intersection^{18,19} to the lower S₁ state ($\tau_2 \approx 100$ fs).²⁰ In contrast, the internal conversion (IC) of S₁ → S₀ is much slower. The S₁ lifetime of **I** varies from 8.5 ps (methanol) to 26.4 ps (3-methylpentane)^{14–17} and that of **II** from 1.9 ps (acetonitrile) to 11.7 ps (3-methylpentane).¹³ The S₁ lifetimes of these molecules are strongly dependent on the solvent polarity, which is generally interpreted as resulting from the increased intramolecular charge transfer character of the S₁ state in polar solvents.^{17,21}

The energy of the S₁ state of carotenoids has been of great interest and has been determined in a variety of ways (see ref

* To whom correspondence should be addressed. Phone: (510) 643-2735. Fax: (510) 642-6340. E-mail: GRFleming@lbl.gov.

[†] Current address: Lawrence Livermore National Laboratory, P.O. Box 808, Livermore, CA 94551-0808.

[‡] Current address: Sandia National Laboratories, P.O. Box 5800, MS 1153, Albuquerque, NM 87185-1153.

11 for a comprehensive set of references): by scanning the $S_1 \rightarrow S_2$ excited-state absorption in the near-infrared region following S_2 excitation,²² by measuring the 2PE spectrum,^{23,24} or by measuring the weak $S_1 \rightarrow S_0$ fluorescence.²⁵ Resonance Raman scattering can also be used to locate the S_1 state by scanning the excitation frequency while monitoring the strong C–C and C=C stretching modes.²⁶ An S_1 energy of ~ 15300 cm^{-1} (653 nm) was estimated for **I** by comparing S_1 lifetimes of several carotenoids with known S_1 levels,¹⁴ and using the energy gap law.²⁷ The S_1 energy of **II** has not been reported, but ~ 14400 cm^{-1} (694 nm) was estimated for a similar apocarotenoid which has the same polyene backbone but only one nitrile group.¹⁴ However, the S_1 state energies of carotenoids determined by the various methods can vary by as much as 1000 cm^{-1} , which seems too large to be simply ascribed to experimental error.¹¹ The coexistence of different conformers in the S_1 excited states has been proposed to explain the difference in the S_1 energy determined via the different methods.²⁸ Recent ab initio calculations¹⁹ and a time-resolved coherent anti-Stokes Raman scattering experiment²⁹ on short polyenes, and fluorescence measurements^{30,31} from the S_1 and S_2 states of dual-emitting carotenoids all support the complex nature of the S_1 singlet excited state.

Direct pumping of S_1 by 2PE and indirect pumping of S_1 via the S_2 state by 1PE may populate different regions on the S_1 potential energy surface. The 1PE-prepared S_1 population is generated by an internal conversion from the S_2 state and subsequent vibrational relaxation to the S_1 state minimum via totally symmetric deformations of the polyene backbone.¹⁹ The S_1 state populated directly by 2PE is free from any interference from the S_2 state. Thus, a comparison of the spectra of the S_1 states prepared by 1PE and 2PE may shed light on the complex nature of the S_1 potential surface. In this study, we present ultrafast infrared absorption measurements of the S_1 excited states of **I** and **II** after excitation of the S_2 and S_1 states by 1PE and 2PE, respectively.

Experimental Methods

The output of a Ti:sapphire oscillator (Femtosource Compact Pro, Femtolasers) was amplified using a regenerative amplifier system (Legend Elite USP, Coherent) to produce ~ 35 fs, ~ 1 mJ pulses centered at 800 nm with a 1 kHz repetition rate. One quarter of the amplifier output is introduced into a mid-infrared (mid-IR) optical parametric amplifier (OPA; home-built) and the rest into another near-infrared OPA (TOPAS 800-fs, Quantronix). The mid-IR OPA, a two-pass β -barium borate (BBO) based near-infrared OPA followed by difference frequency generation in a AgGaS₂ crystal, produces ~ 100 fs, 2 μJ mid-IR probe pulses tunable between 1250 and 3000 cm^{-1} .^{32,33} A near-infrared OPA (TOPAS) produces ~ 60 fs, ~ 100 μJ pulses in the tuning range of 1150–2600 nm. The signal pulse of the TOPAS in the 1150–1500 nm range was used directly for the pump in the 2PE experiment. Visible pump pulses (60–80 fs, ~ 5 μJ) in the 470–520 nm range for 1PE experiments were produced by mixing the signal of the TOPAS with the residual 800 nm pump in a type I 1.0 mm BBO crystal followed by a prism pair compressor.

The mid-IR probe pulses were separated into a signal and reference at a ZnSe beamsplitter and focused using an off-axis parabolic mirror ($f = 10$ cm with a 150–200 μm focal spot). The pump pulses were focused with a separate lens to match the focal spot size of the probe pulses. The signal and reference probe pulses were collimated using an identical parabolic mirror, spectrally resolved using a Triax 190 imaging spectrograph

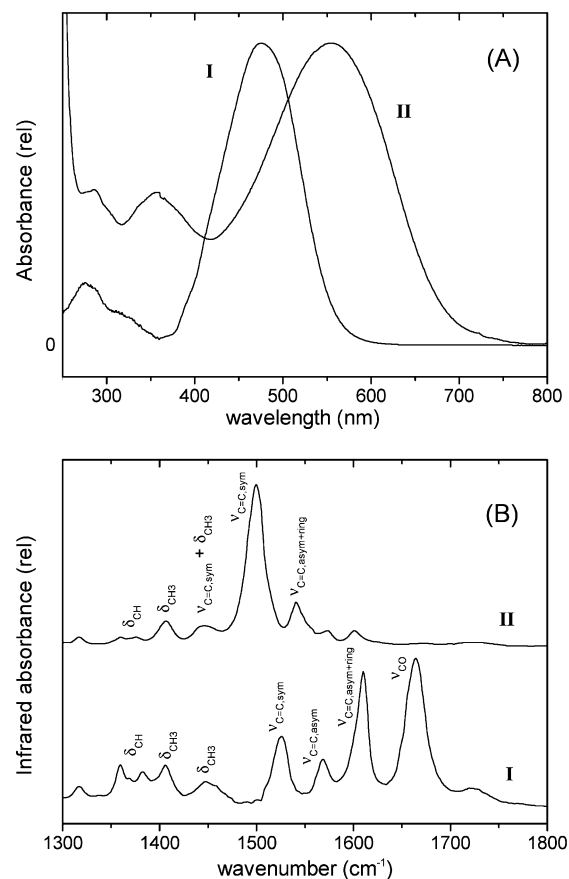


Figure 2. (A) Steady-state absorption spectrum of **I** ($\lambda_{\max} = 475$ nm) and **II** ($\lambda_{\max} = 560$ nm) in chloroform. (B) FT-IR spectra of **I** and **II** in chloroform with solvent peaks subtracted. Vibrational assignments of major absorption bands are displayed.

(HORIBA Jobin Yvon), and detected using two arrays of a 32-element HgCdTe detector (IR-6416, InfraRed Associates). With a 150 gr/mm grating, a spectral resolution of 2–4 cm^{-1} per pixel (increasing from 1250 to 1850 cm^{-1}) was obtained.

8'-Apo- β -caroten-8'-al (**I**) was purchased from Sigma-Aldrich, and 7',7'-dicyano-7'-apo- β -carotene (**II**) was a gift from Lowell Kispert at the University of Alabama.¹³ Apocarotenoids **I** and **II** and the solvents purchased from Sigma-Aldrich or Cambridge Isotope Laboratories were used without further purification. Sample concentrations were 0.5 g/L (1.2 mM for **I**, 1.1 mM for **II**) for 1PE, where an optical absorption of ~ 1.0 at $\lambda_{\max} = 475$ nm (**I**) and 560 nm (**II**) was obtained from a 0.25 mm path length. Solutions with concentration of 2.0 g/L (4.8 mM for **I**, 4.3 mM for **II**) were used for 2PE experiments. Dilution to 10^{-5} M did not change the steady-state absorption spectra of **I** and **II**. A flowing sample cell with two CaF₂ windows separated by a 0.25 mm thick Teflon spacer was used to circulate the sample, and all the measurements were done at ambient temperature.

Results

Electronic and Vibrational Spectra. Figure 2A shows the steady-state absorption spectra of **I** and **II** in chloroform solution. The main absorption band of **II** ($\lambda_{\max} = 560$ nm, 170 nm fwhm) in chloroform is broader and red-shifted compared to that of **I** ($\lambda_{\max} = 475$ nm, 100 nm fwhm). Population of S_2 of **I** and **II** by 1PE was obtained by pumping at 490 and 508 nm, respectively, and direct pumping of the S_1 states of **I** and **II** by 2PE used 1275 and 1400 nm pump pulses, respectively. The 2PE wavelengths were selected to maximize the initial difference

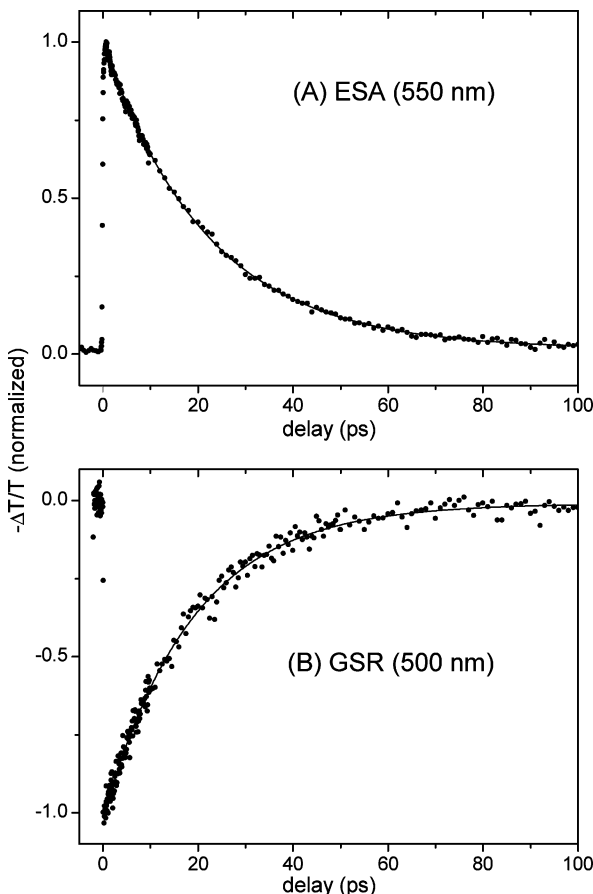


Figure 3. (A) Kinetic trace of the ESA ($S_1 \rightarrow S_N$) of **I** in chloroform at 550 nm following 1PE at 490 nm. (B) Kinetic trace of the GSR of **I** in chloroform at 500 nm following 1PE at 500 nm. Kinetic data are shown as dots, and the exponential fits are shown as lines.

infrared absorptions of these apocarotenoid molecules, and values equal to 2 times the energies of 2PE photons (15690 cm^{-1} or 638 nm for **I** and 14300 cm^{-1} or 700 nm for **II**) were close to the estimated S_1 levels.¹⁴ There is no absorption around 638 nm for **I** where 2PE was applied, whereas **II** has some absorption at 700 nm. We expect 2PE at 1400 nm to only excite the S_1 state of **II** because of the selection rule. Figure 2B displays the FT-IR spectra of **I** and **II** in chloroform solution. A strong peak at 1669 cm^{-1} in the spectrum of **I** is $\nu_{\text{C=O}}$, and three $\nu_{\text{C=C}}$ peaks with split intensities at 1524, 1568, and 1611 cm^{-1} are also identified. Three $\nu_{\text{C=C}}$ peaks at 1444, 1500, and 1541 cm^{-1} exist in the spectrum of **II**, but the symmetric stretch at 1500 cm^{-1} is the most intense. Separate bands at 1573 and 1601 cm^{-1} are not identified but can be tentatively assigned as asymmetric $\nu_{\text{C=C}}$. The bending modes appearing at 1405 and 1446 cm^{-1} in **I** and 1407 cm^{-1} in **II** are CH_3 deformation modes, and another group of bands at 1357 and 1380 cm^{-1} in **I** and 1361 and 1377 cm^{-1} in **II** are CH in-plane bending modes. These vibrational assignments are based on previous resonance Raman studies^{12,34,35} and DFT simulation results. Details of our DFT simulations for various conformers of **I** and **II** in the ground state will be discussed in a subsequent paper.³⁶

Figure 3 displays transient absorption kinetic traces and exponential fits for **I** in chloroform solution following 1PE. Fit parameters for all the data in Figure 3 are collected in Table 1. Figure 3A shows the kinetics of the $S_1 \rightarrow S_N$ excited-state absorption (ESA) measured at 550 nm¹⁴ following 1PE at 490 nm. The fit shows a single-exponential decay with a 19.3 ps time constant corresponding to the S_1 lifetime. In Figure 3B,

TABLE 1: Kinetics of $S_1 \rightarrow S_N$ Excited-State Absorption and the Ground-State Recovery of 8'-Apo- β -caroten-8'-al

solvent	a_s^a	τ_s^b (ps)	a_1^a	τ_1 (ps)
$S_1 \rightarrow S_N$ ESA ^c				
CHCl ₃	1.00	19.3		
GSR ^d				
CCl ₄	0.38	0.27	0.62	27.2
CDCl ₃	0.20	0.24	0.80	19.3
CHCl ₃	0.55	0.28	0.45	18.6

^a Amplitudes are in arbitrary units. ^b Solvent spikes. ^c ESA of **I** measured at 550 nm following 1PE at 490 nm. ^d GSR of **I** measured at 500 nm following 1PE at 500 nm.

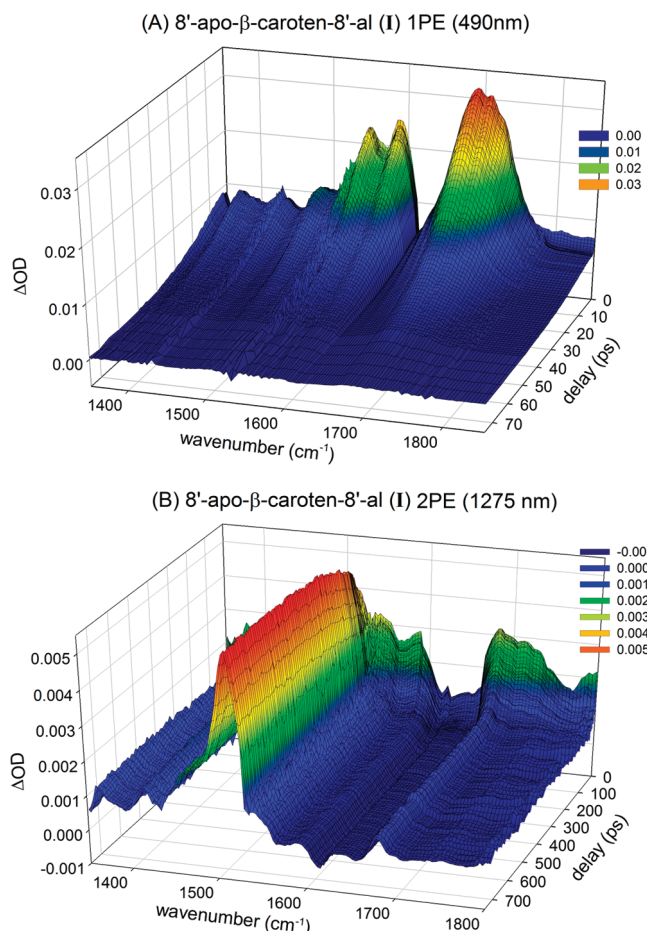


Figure 4. Surface plots of the excited-state infrared absorption for **I** in chloroform shown as a function of time following (A) 1PE at 490 nm and (B) 2PE at 1275 nm.

the ground-state recovery (GSR) trace at a 500 nm probe following 1PE at 500 nm is shown, where a single-exponential lifetime ($\tau_1 = 18.6$ ps) is obtained as well as a fast solvent spike ($\tau_s \approx 0.25$ ps, observed in all solvents). The GSR results of **I** in carbon tetrachloride ($\tau_1 = 27.2$ ps) and chloroform-*d* ($\tau_1 = 19.3$ ps) are also given in Table 1.

8'-Apo- β -caroten-8'-al. Figure 4 displays surface plots of the transient infrared absorption for **I** in chloroform solution in the mid-IR frequency range of 1350–1850 cm^{-1} following (A) 1PE at 490 nm and (B) 2PE at 1275 nm (note that the time axes of the two plots differ). The surface plots were constructed by measuring the difference infrared spectrum of **I** with and without a pump pulse at each delay time. The excited-state spectra and dynamics of **I** are completely different between 1PE and 2PE: all the excited-state absorptions of **I** decay to the ground state with the S_1 lifetime for 1PE, but a group of bands

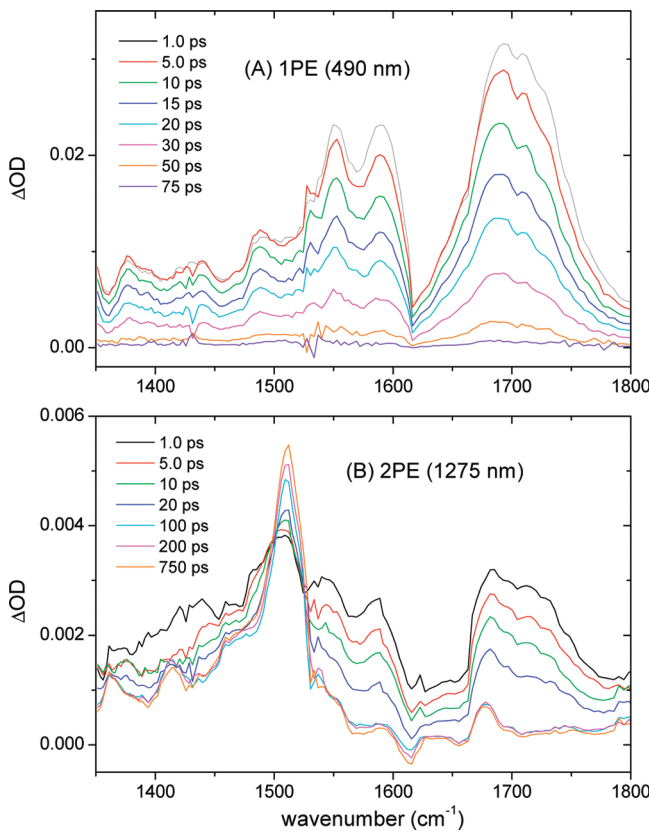


Figure 5. Transient infrared spectra of **I** in chloroform in (A) 1PE at 490 nm and (B) 2PE at 1275 nm taken from the surface plots in Figure 4.

including a very strong peak at 1510 cm^{-1} show no decay out to 1 ns for 2PE, the limit of our translation stage. Transient infrared spectra of **I** at multiple delay times, taken from the surface plots in Figure 4, are shown in Figure 5 for better comparison. The 1PE spectrum in Figure 5A shows a strong band at $1670\text{--}1730\text{ cm}^{-1}$, another group of medium-strong bands at 1488 , 1550 , and 1585 cm^{-1} , and weak bands at 1378 and 1439 cm^{-1} . All these bands have essentially zero amplitudes at 75 ps, as clearly seen in Figure 4A. All these absorption bands have a nearly instrument response limited rise and a single-exponential decay of ~ 19.4 ps (fit parameters for 1585 and 1683 cm^{-1} are shown in Table 2). No major changes in bandwidth or frequency during the decay are detected. This 19.4 ps lifetime is very close to the 19.3 and 18.6 ps S_1 lifetimes of **I** obtained in the $S_1 \rightarrow S_N$ ESA and GSR experiments, respectively (Figure 3 and Table 1).

In the 2PE spectrum of **I** in Figure 5B, the most intense absorption band is at 1510 cm^{-1} , which is not evident in the 1PE case and has a distinct temporal pattern from other major bands in both the 2PE and 1PE spectra. The intensity of this band increases over time and has not decayed by 1 ns delay. Next to this strong long-lived band, there are bands at 1544 and 1588 cm^{-1} , and a strong band at $1670\text{--}1730\text{ cm}^{-1}$ which is composed of two or more sub-bands. The kinetics of all the major infrared absorption bands measured in 2PE were fit with a few exponential rises or decays, and these fit parameters are collected in Table 2. Fit results of the long-lived band at 1508 cm^{-1} for **I** in carbon tetrachloride with 2PE at 1275 nm are also included for comparison. The majority of the bands (1544 , 1588 , and 1730 cm^{-1}) in the 2PE spectra decay with a single time constant of ~ 17 ps except for the 20.2 ps found for the peak at 1678 cm^{-1} , which results from the appearance of a long-

lived absorption at the same frequency. The ~ 17 ps lifetime is about 10% faster than the S_1 lifetime of 19.4 ps found in the 1PE. The long-lived band at 1510 cm^{-1} shows two exponential rises, with time constants of 15.4 and 142 ps in chloroform. Other long-lived bands at 1363 , 1415 , and 1678 cm^{-1} and a ground-state bleach appearing at 1614 cm^{-1} have not decayed by the 1 ns experimental time limit. A good estimate of the lifetime from these bands was not possible because of the small amplitude and nearby strong S_1 bands. The 2PE data for **I** in carbon tetrachloride solution with 1275 nm pumping show a single-exponential rise of the 1508 cm^{-1} band with a time constant of 16.8 ps and a single-exponential decay with a 342 ps time constant as listed in Table 2.

7',7'-Dicyano-7'-apo- β -carotene. Surface plots of the transient infrared absorption for **II** in chloroform solution in the mid-IR frequency range of $1250\text{--}1750\text{ cm}^{-1}$ following (A) 1PE at 508 nm and (B) 2PE at 1400 nm are shown in Figure 6. The time axes and the frequency axes of two plots differ. These surface plots were constructed in the same manner as for Figure 4. The excited-state spectra and dynamics of **II** are distinct for 1PE and 2PE. All the excited-state infrared absorptions of **II** decay to the ground state in about 10 ps in 1PE except a dispersive peak and bleach pattern at $1480\text{--}1510\text{ cm}^{-1}$ which disappears in 50 ps. However, with 2PE a group of bands including a very strong peak at 1507 cm^{-1} last longer than 1 ns and do not show decay. Transient infrared spectra at multiple delay times taken from the surface plots in Figure 6 are shown in Figure 7. Exponential fit parameters for all major bands in 1PE and 2PE are collected in Table 3. The 1PE spectrum of **II** has its most intense peaks at 1605 , 1630 , and 1665 cm^{-1} , a ground-state bleach at 1508 cm^{-1} , and weaker peaks at 1432 , 1462 , 1482 , 1524 , and 1544 cm^{-1} . All of these absorption bands have a nearly instrument response limited rise, and a single-exponential decay of ~ 2.0 ps, which is assigned as the S_1 lifetime (for the potential minimum reached from S_2) of **II** in chloroform. Excited-state absorption at 1482 cm^{-1} and ground-state bleach at 1508 cm^{-1} have an additional 12 ps decay component in addition to the ~ 2.0 ps S_1 lifetime. This can be explained as the formation of a hot-ground-state band at 1482 cm^{-1} overlapped with the S_1 band at the same position. The existence of intense neighbor S_1 bands at 1482 and 1524 cm^{-1} makes it difficult to estimate the depth of the ground-state bleach at 1508 cm^{-1} at earlier delay times. This is the reason why we observe a 2.0 ps rise component (decreased ΔOD , the definition of rise/decay is opposite for the bleach band) instead of a decay from the kinetic trace of the 1508 cm^{-1} bleach. Formation of vibrationally hot molecules in the ground state, which dissipates the excess energy to the surrounding solvent in ~ 12 ps, is not present in the data of **I** since the S_1 lifetime is about 10 times longer than that of **II** in chloroform. A similar hot-ground-state dispersive pattern was observed for **II** in acetonitrile- d_3 solution with 1PE where the S_1 lifetime is extremely short (0.50 ± 0.01 ps) and the decay lifetime of hot-ground-state bands is 8.2 ± 0.1 ps. The S_1 lifetime of **II** in carbon tetrachloride is 9.1 ± 0.1 ps with 1PE, and the hot-ground-state bands were not observed. The fact that these types of bands are only seen when the S_1 lifetime is shorter than ~ 2 ps supports the assignment of the 1482 cm^{-1} peak as the symmetric C=C stretching mode in the hot ground state. All the bands in the 1PE spectrum of **II** (except the hot-ground-state bands) decay to almost zero in 10 ps. The S_1 lifetime of **II** in acetonitrile- d_3 was reported by Kispert and co-workers¹³ as 1.9 ± 0.5 ps, but the laser pulses used in the experiment were too long ($2\text{--}4$ ps) to resolve the fast lifetime.

TABLE 2: Kinetics of the Excited-State Infrared Absorption of 8'-Apo- β -caroten-8'-al

frequency (cm^{-1})	a_1^a	τ_1 (ps)	a_2^a	τ_2 (ps)	a_3^a	τ_3 (ps)	a_4^a	τ_4 (ps)			
				1PE, CHCl_3							
1585			1.00	19.4 \pm 0.2							
1683			1.00	19.4 \pm 0.2							
				2PE, CHCl_3							
1415	0.27	3.0 \pm 1.1		-0.33	15.4 \pm 2.4	-0.53	341 \pm 75	-0.73	619 \pm 98		
1510				0.82	16.6 \pm 2.6	-0.67	142 \pm 9				
1544	0.18	2.5 \pm 0.9		1.00	17.2 \pm 0.4						
1588						0.27	241 \pm 43				
1614	0.73	8.8 \pm 0.4		1.00	20.2 \pm 0.4	0.08	107 \pm 30				
1678 ^b				0.92	16.2 \pm 1.9						
1730											
				2PE, CCl_4							
1508			-0.72	16.8 \pm 0.9	1.00	342 \pm 24					

^a Amplitudes are in arbitrary units, and positive amplitudes represent decays and negative ones rises. ^b The exact lifetime of this peak could not be determined because of the long-lived absorption appearing at the same frequency.

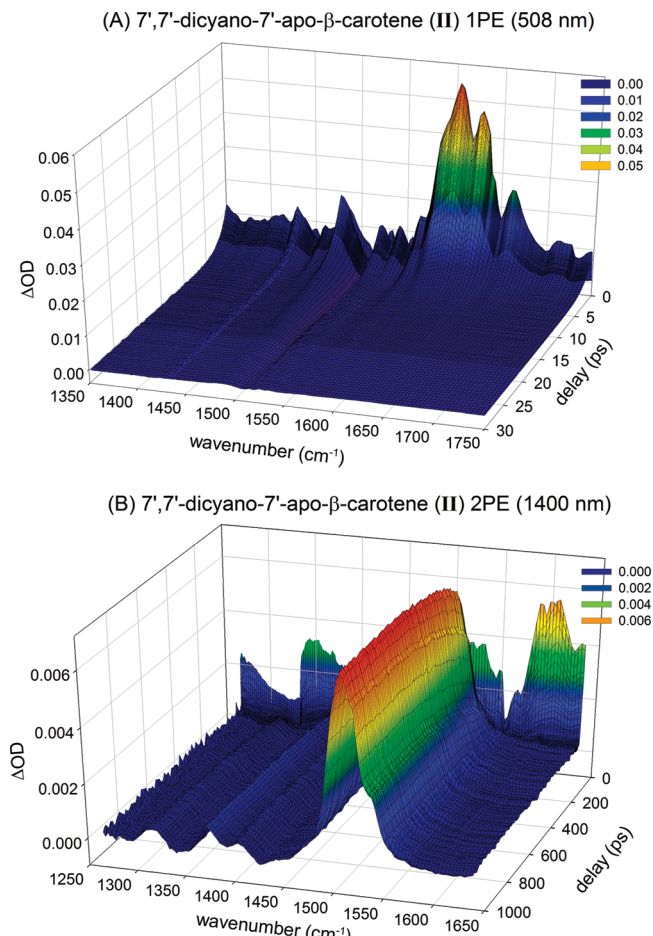


Figure 6. Surface plots of the excited-state infrared absorption for **II** in chloroform shown as a function of time following (A) 1PE at 508 nm and (B) 2PE at 1400 nm.

The 2PE spectrum exhibits more complicated dynamics. The most intense band is the absorption at 1507 cm^{-1} , which is not evident in the 1PE spectrum and has a distinct kinetic pattern from other major bands in 2PE and 1PE. The 1507 cm^{-1} band shows a two-exponential rise, with time constants of 16.5 and 233 ps in chloroform. Other long-lived bands at 1316, 1373, and 1405 cm^{-1} show similar two-exponential rises in addition to S_1 decay, but exponential fits to these bands are not very good due to the low signal amplitudes. Another set of strong

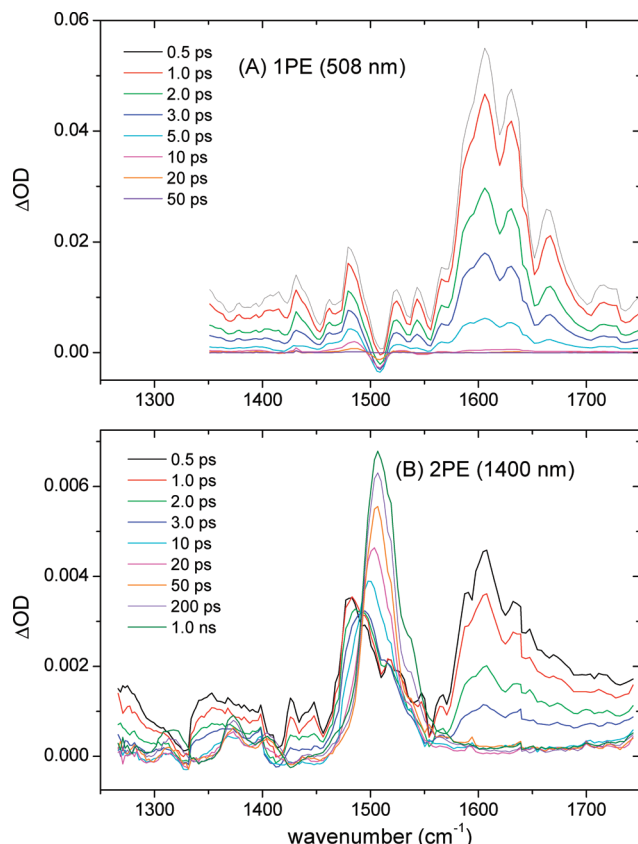


Figure 7. Transient infrared spectra of **II** in chloroform in (A) 1PE at 508 nm and (B) 2PE at 1400 nm taken from the surface plots in Figure 6.

bands at 1427, 1482, and 1606 cm^{-1} which disappear completely in ~ 10 ps show a single-exponential decay with a ~ 1.7 ps time constant. This ~ 1.7 ps time constant is assigned to the S_1 lifetime in the potential minimum reached with 2PE.

The formation of a long-lived triplet excited state of β -carotene from singlet excited states by multiphoton excitation of near-infrared pulses was reported by Motzkus and co-workers recently.³⁷ We checked whether the transient infrared absorptions measured with 2PE have any contribution of multiphoton excitation. Figure 8 shows the pump power dependence of two infrared absorption intensities for **I** in chloroform in the 2PE spectra pumped at 1275 nm. The plus signs represent the most

TABLE 3: Kinetics of the Excited-State Infrared Absorption of 7',7'-Dicyano-7'-apo- β -carotene

frequency (cm ⁻¹)	a_1^a	τ_1 (ps)	a_2^a	τ_2 (ps)	a_3^a	τ_3 (ps)
1PE, CHCl ₃						
1432	1.00	2.0 ± 0.1				
1482	0.79	1.9 ± 0.1	0.21	11.0 ± 0.2		
1508	-1.00	2.0 ± 0.1	0.72	12.5 ± 0.2		
1605	1.00	2.0 ± 0.1				
1PE, CD ₃ CN						
1595	1.00	0.50 ± 0.01				
1PE, CCl ₄						
1642	1.00	9.1 ± 0.1				
2PE, CHCl ₃						
1316	1.00	1.5 ± 0.1	-0.26	19.1 ± 5.6	-0.59	254 ± 24
1373	1.00	1.1 ± 0.1	-0.06	29.5 ± 7.5	-0.37	204 ± 23
1427	1.00	1.7 ± 0.1				
1482	1.00	1.7 ± 0.1				
1507			-0.71	16.5 ± 0.5	-0.29	233 ± 7
1606	1.00	1.7 ± 0.1				

^a Amplitudes are in arbitrary units, and positive amplitudes represent decays and negative ones rises.

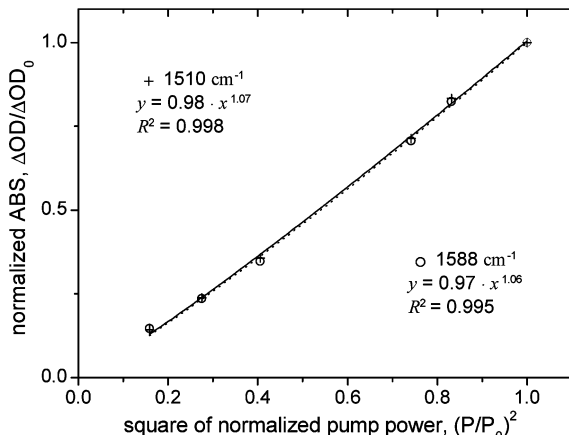


Figure 8. Pump power dependence of two infrared absorption bands at 1510 cm⁻¹ (plus signs with dotted line) and 1588 cm⁻¹ (circles with solid line) of **I** in chloroform with 2PE (1275 nm). The intensities of the long-lived absorption at 1510 cm⁻¹ are taken at a 750 ps delay, and those of the S₁ band at 1588 cm⁻¹ are taken at a 1 ps delay. Power fits to the data show two-photon behavior on the signal strength for both bands.

intense, long-lived band at 1510 cm⁻¹ in the 2PE spectrum, whose intensity was measured at 750 ps delay. The circles represent the 1588 cm⁻¹ band, which appears in both 1PE and 2PE spectra and decays with an S₁ lifetime of ~17 ps in 2PE. The intensity of the 1588 cm⁻¹ band was measured at a 1 ps delay to minimize the contribution of a long-lived absorption band. The ordinate is the normalized absorbance ($\Delta OD/\Delta OD_0$), and the abscissa is the square of the normalized pump power [$(P/P_0)^2$]. Both power dependence fits are approximately linear (1.06–1.07) with the square of the pump power which shows the two-photon excitation dependences of both absorption bands. From this result we exclude the participation of a higher singlet excited state by multiphoton excitation processes in the 2PE case and conclude that the S₁ population is created by the direct two-photon absorption from S₀ to S₁.

Discussion

The nature of the S₁ potential surface of **I** and **II** allows distinct populations prepared by 1PE or by 2PE that do not

communicate on the time scale of the S₁ lifetime. In chloroform solution, the 1PE-prepared population returns to the original ground-state position on a ~19 ps (**I**) and a ~2.0 ps (**II**) time scale, whereas the 2PE-prepared population decays from the S₁ state on a ~17 ps (**I**) and a ~1.7 ps (**II**) time scale but does not directly return to the fully relaxed ground state. The long-lived absorption bands observed even after the completion of S₁ decay in 2PE experiments of **I** and **II** are not observed in 1PE where the S₁ population is created via S₂. The differences in the S₁ lifetimes in addition to the S₁ spectra of **I** and **II** between 1PE and 2PE can be explained by the existence of multiple conformations in the S₁ potential surface as suggested by Polívka et al.²⁸ In this paper, we discuss the population dynamics and the infrared spectrum of the S₁ excited state only and reserve the discussion of the long-lived absorptions for a subsequent paper.

S₁ Spectra: Intensity. The infrared absorptions of **I** and **II** in the S₁ state following 1PE are very intense compared to the ground-state absorption bands. For example, **I** in the ground state shows maximum infrared absorbances of 0.022 at 1669 cm⁻¹ ($\nu_{C=O}$) and 0.018 at 1611 cm⁻¹ ($\nu_{C=C, \text{asym+ring}}$) with a 0.5 g/L chloroform solution in a 0.25 mm thick sample cell. In 1PE experiments, a maximum transient infrared absorbance of 0.032 at 1683 cm⁻¹ was measured, which is larger than any absorbance observed in the ground state. The S₁ state of **I** is estimated to have ~7.2 times larger infrared activity than the ground state by comparing the maximum absorbances around 1669 (S₀ $\nu_{C=O}$) and 1683 cm⁻¹ (S₁). The number of **I** molecules in the excitation volume was 5.68×10^{12} , which were excited by 1.23×10^{12} photons at 490 nm. About 20% of the **I** molecules were excited by the pump pulse according to the measured absorbance of 1.16 at 490 nm. The S₁ state of **II** also showed ~3.3 times greater infrared absorption strength compared to the ground state. The infrared absorptions of **I** and **II** in the S₁ state measured following 2PE are weak; they are an order of magnitude smaller in intensity compared to those in 1PE experiments although 100 times combined increases in the sample concentration and the number of photons were used for 2PE experiments. The extinction coefficients for two-photon absorption ($S_0 \rightarrow S_1$) of **I** and **II** at 1275 and 1400 nm, respectively, are estimated to be ~ 10^{-3} times smaller than those of the one-photon absorption ($S_0 \rightarrow S_2$).

The infrared absorption intensity is dependent on the square of the partial derivative of the transition dipole moment with respect to a normal mode coordinate. The increased infrared activities in the S₁ excited states for **I** and **II** in the 1PE experiment can be explained by the changes in the molecular dipole moment of these molecules in the S₁ excited state. The change in the dipole moments between the ground and the singlet excited states of carotenoids have been measured by Stark effect spectroscopy,^{38,39} where $\Delta\mu = 3-5$ D for symmetric carotenoids and larger changes for the polarized carotenoids were observed. The gas-phase dipole moments of the asymmetric apocarotenoids including **I** ($\Delta\mu = 2.82$ D for $S_0 \rightarrow S_1$) and **II** ($\Delta\mu = 5.06$ D for $S_0 \rightarrow S_1$) are estimated to increase in the S₁ state relative to the ground state by AM1 semiempirical molecular orbital calculations.^{13,15}

Vibrational Assignments of the S₁ Bands. The symmetric $\nu_{C=C}$ band of β -carotene and **I** in the S₁ excited state has been shown to split into two bands in various time-resolved Raman scattering experiments.⁴⁰⁻⁴⁴ The small blue shifts (~20 cm⁻¹ from the ground-state positions) of the S₁ $\nu_{C=C}$ bands appearing at 1543 and 1526 cm⁻¹ for β -carotene and **I**, respectively, are explained as arising from a bond order decrease in the excited

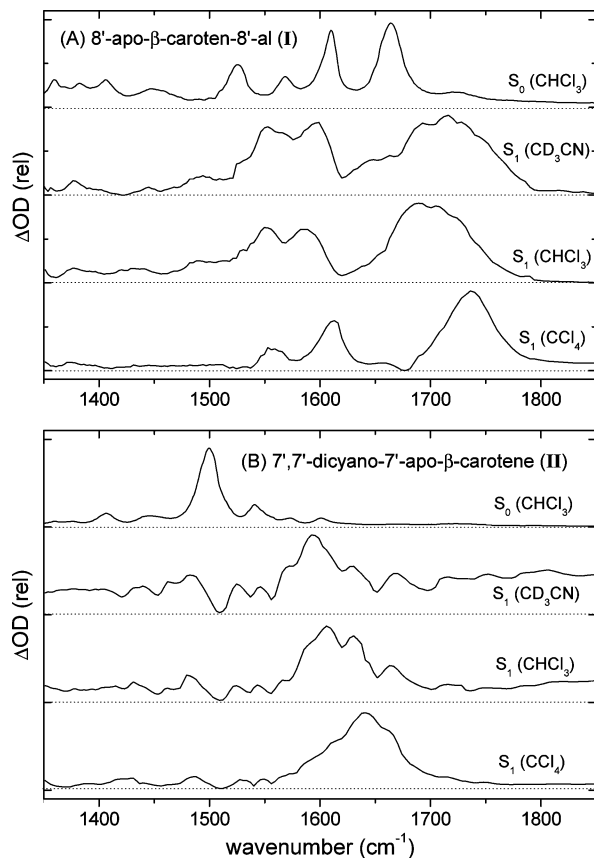


Figure 9. Excited-state infrared absorption spectra of (A) **I** at 1.0 ps and (B) **II** at 0.5 ps after 1PE of 490 and 508 nm, respectively, in solutions of acetonitrile-*d*₃, chloroform, and carbon tetrachloride. The ground-state FT-IR spectra of **I** and **II** in chloroform solution are also shown in the top section of each graph. Each spectrum was normalized for comparison, and the zero absorbance line of each spectrum is shown as a dotted line.

state. However, substantial blue shifts ($\sim 260 \text{ cm}^{-1}$ for β -carotene and $\sim 190 \text{ cm}^{-1}$ for **I**⁴⁰) in the S₁ excited state for the symmetric $\nu_{\text{C}=\text{C}}$ bands appearing at 1781 and 1713 cm^{-1} for β -carotene and **I**, respectively, are explained using a diabatic vibronic coupling model,¹⁰ where the frequency of the Franck-Condon active totally symmetric (a_g) C=C stretching mode is increased upon S₁ excitation due to strong vibronic coupling between the S₀ and S₁ states. The smaller blue shift of $\nu_{\text{C}=\text{C}}$ for **I** ($\sim 190 \text{ cm}^{-1}$) compared to the highly symmetric β -carotene was then explained with an increased vibronic coupling between the S₁ and S₂ states in polarized carotenoids, which offsets the large blue shifts arising from the vibronic coupling between the S₀ and S₁ states.⁴⁰ It is known that similar blue shifts have also been observed from non totally symmetric vibrational modes of benzene or naphthalene.⁴⁵⁻⁴⁷

Vibrational modes of **I** and **II**, either of a' (symmetric) or a'' (asymmetric) symmetry in the C_s point group, are all infrared active. Vibrational assignments of the $\nu_{\text{C}=\text{C}}$ modes for apocarotenoids **I** and **II** in the S₁ excited state are based on the peak splitting and frequency shifts similarly observed in the Raman experiments. Figure 9 shows the transient infrared spectra of (A) **I** at a 1.0 ps delay at a 490 nm pump and (B) **II** at a 0.5 ps delay at a 508 nm pump in various solvents as well as the ground-state FT-IR spectra. The S₁ vibrational frequencies and vibrational assignments of $\nu_{\text{C}=\text{C}}$ and $\nu_{\text{C}=\text{O}}$ for **I** and **II** are summarized in Table 4.

From the S₁ spectra of **II** in Figure 9B, two groups of $\nu_{\text{C}=\text{C}}$ bands are identified. A group of $\nu_{\text{C}=\text{C}}$ bands in the 1550–1650

TABLE 4: Vibrational Assignments of 8'-Apo- β -caroten-8'-al and 7',7'-Dicyano-7'-apo- β -carotene in the S₀ and S₁ States^a

assignment	solvent	$\tilde{\nu}_{\text{S}0}$	$\tilde{\nu}_{\text{S}1}(\text{RS})^b$	$\tilde{\nu}_{\text{S}1}(\text{BS})^c$
$\nu_{\text{C}=\text{C},\text{sym}}$	8'-Apo- β -caroten-8'-al (I)			
	CD ₃ CN	1492		
	CH ₃ Cl	1524	1488	
	CCl ₄			
$\nu_{\text{C}=\text{C},\text{asym}}$	CD ₃ CN	1553		
	CH ₃ Cl	1568	1550	
	CCl ₄		1560	
	CD ₃ CN	1600		
$\nu_{\text{C}=\text{C},\text{asym+ring}}$	CH ₃ Cl	1611	1585	
	CCl ₄		1612	
	CD ₃ CN			~1715
	CH ₃ Cl	1669		~1683
$\nu_{\text{C}=\text{O}}$	CCl ₄			~1739
	CD ₃ CN			
	CH ₃ Cl			
	CCl ₄			
7',7'-Dicyano-7'-apo- β -carotene (II)				
$\nu_{\text{C}=\text{C},\text{sym}} + \delta_{\text{CH}_3}$	CD ₃ CN	1444	~1437	~1572
	CH ₃ Cl		~1435	~1567/1589
	CCl ₄		~1430	~1613
	CD ₃ CN	1500	1484	1595
$\nu_{\text{C}=\text{C},\text{sym}}$	CH ₃ Cl		1482	1605
	CCl ₄		1487	1642
	CD ₃ CN		1527	1630
	CH ₃ Cl	1541	1524	1630
$\nu_{\text{C}=\text{C},\text{asym+ring}}$	CCl ₄		1531	~1688
	CD ₃ CN		1547	1669
	CH ₃ Cl	1573	1544	1665
	CCl ₄		1549	~1717

^a All frequencies are in units of cm^{-1} , and all the excited-state frequencies are measured from the 1PE results. ^b Frequencies of red-shifted bands in the S₁ state. ^c Frequencies of blue-shifted bands in the S₁ state. The exact locations of blue-shifted $\nu_{\text{C}=\text{C}}$ and $\nu_{\text{C}=\text{O}}$ cannot be determined, but the center of the intense blue-shifted band is estimated as the location of $\nu_{\text{C}=\text{O}}$. ^d The identity of this band is not confirmed but assumed to be one of the asymmetrical $\nu_{\text{C}=\text{C}}$ bands of the S₁ state.

cm^{-1} region with $\sim 100 \text{ cm}^{-1}$ blue shifts show several times larger absorption strengths and broader bandwidths than the ground-state bands. However, the second group of $\nu_{\text{C}=\text{C}}$ bands in the 1450–1550 cm^{-1} region show smaller red shifts ($\sim 20 \text{ cm}^{-1}$) from the ground-state positions and have smaller absorption strengths and narrower bandwidths than the blue-shifted $\nu_{\text{C}=\text{C}}$ bands for the S₁ state. Each group of $\nu_{\text{C}=\text{C}}$ bands include three or four symmetric and asymmetric $\nu_{\text{C}=\text{C}}$ modes partly mixed with δ_{CH_3} or ring stretching (refer to Table 4 for detailed vibrational assignments).

In the S₁ excited-state spectra of **I** in Figure 9A, exact vibrational assignments were not possible especially in the 1630–1770 cm^{-1} region due to the coexistence of strong $\nu_{\text{C}=\text{O}}$ and $\nu_{\text{C}=\text{C}}$ modes. A strong band centered at 1739, 1715, and 1690 cm^{-1} in CCl₄, CD₃CN, and CHCl₃, respectively, was assigned as $\nu_{\text{C}=\text{O}}$ in the S₁ state since $\nu_{\text{C}=\text{O}}$ is the strongest band in the ground state and would be expected to be the strongest band in the excited state. In addition, the breadth of this intense band and the spectra of **II** (where the C≡N band is shifted to 2217 cm^{-1}) show that there are substantial contributions from the $\nu_{\text{C}=\text{C}}$ bands in the S₁ excited state in this region, although the exact location of the blue-shifted symmetric and asymmetric $\nu_{\text{C}=\text{C}}$ modes in this region cannot be resolved. Similar blue shifts of $\sim 100 \text{ cm}^{-1}$ from the ground-state positions for $\nu_{\text{C}=\text{C},\text{asym}}$ are estimated from the major peak positions in the 1630–1770 cm^{-1} region of the S₁ state spectra of **I**. The blue shifts for $\nu_{\text{C}=\text{O}}$ in the S₁ state are estimated to be 25–60 cm^{-1} . Three red-shifted

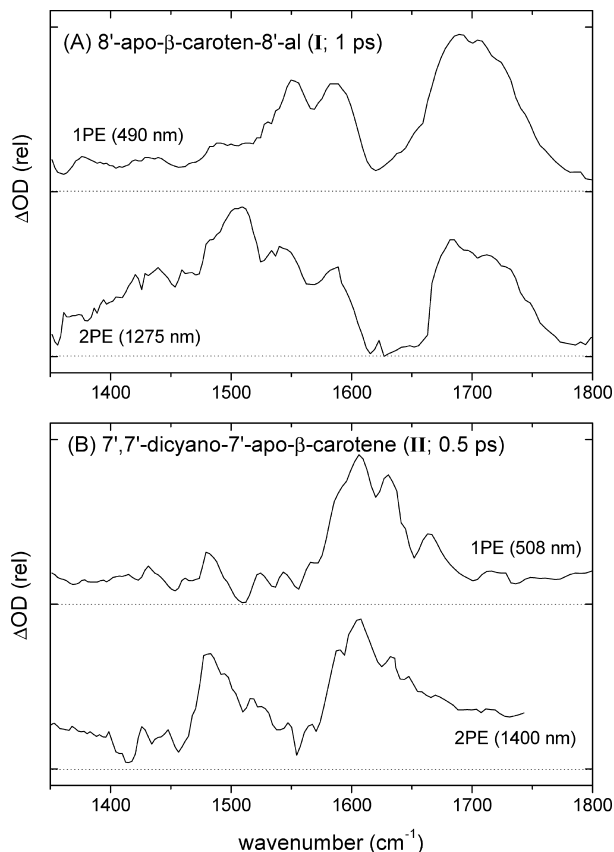


Figure 10. Excited-state infrared absorption spectra of (A) **I** at 1.0 ps and (B) **II** at 0.5 ps after 1PE and 2PE in chloroform solution. Each spectrum was taken from Figures 5 and 7 and normalized for comparison, and the zero absorbance line of each spectrum is shown as a dotted line.

(20–30 cm⁻¹) $\nu_{\text{C}=\text{C}}$ modes are also identified in the 1450–1630 cm⁻¹ region of the S_1 infrared spectra of **I**.

The relative intensities of three red-shifted $\nu_{\text{C}=\text{C}}$ bands in the S_1 state for **I** and **II** are quite different from those in the ground state (see Figure 9). The asymmetric $\nu_{\text{C}=\text{C}}$ mode of **I** around 1550–1560 cm⁻¹ gains a substantial strength in the S_1 state, whereas the symmetric $\nu_{\text{C}=\text{C}}$ mode of **I** around 1490 cm⁻¹ has a strength similar to that in the ground state. The decrease of the relative intensity of the symmetric $\nu_{\text{C}=\text{C}}$ mode of **II** around 1482 cm⁻¹ in the S_1 state is also obvious. These spectral changes clearly raise the possibility of a change in the conformation of **I** and **II** in the S_1 excited state such as a twist of the polyene backbone of the molecule out of the plane with a concomitant increase in the molecular dipole moment of the S_1 state.

S₁ Spectra: 1PE vs 2PE. Figure 10 displays the infrared spectra of the S_1 state prepared by 1PE and 2PE for (A) **I** and (B) **II** in chloroform at 1.0 and 0.5 ps delay, respectively. These spectra were taken from Figures 5 and 7, and the intensities were normalized for comparison. Time delays of 1.0 or 0.5 ps were chosen to minimize the interference of long-lived absorptions in the 2PE case.

The S_1 spectra of **I** in Figure 10A show clear differences between 1PE and 2PE. An intense group of bands at 1630–1770 cm⁻¹, assigned as $\nu_{\text{C}=\text{O}}$ and $\nu_{\text{C}=\text{C}}$ of the S_1 state, are very similar in both 1PE and 2PE in terms of overall bandwidth (~ 80 cm⁻¹ fwhm) and peak shape. The $\nu_{\text{C}=\text{C}}$ bands in the 1450–1630 cm⁻¹ range also have similar peak positions in the 1PE and 2PE cases, $\nu_{\text{C}=\text{C},\text{sym}}$ at ~ 1490 cm⁻¹, $\nu_{\text{C}=\text{C},\text{asym}}$ at 1545–1550 cm⁻¹, and $\nu_{\text{C}=\text{C},\text{asym+ring}}$ at 1585 cm⁻¹. However, the relative intensities between these $\nu_{\text{C}=\text{C}}$ bands are quite different in the 1PE and

2PE cases such that the symmetric $\nu_{\text{C}=\text{C}}$ is increased a few times in 2PE with respect to the asymmetric $\nu_{\text{C}=\text{C}}$ bands, becoming even larger than the blue-shifted $\nu_{\text{C}=\text{C}}$ and $\nu_{\text{C}=\text{O}}$ bands in the 2PE spectrum of **I**. The δ_{CH_3} (deformation) band at 1440 cm⁻¹ is seen in 1PE and 2PE, but the overall spectral shape below 1450 cm⁻¹ is also quite different between 1PE and 2PE. Although blue-shifted $\nu_{\text{C}=\text{C}}$ and $\nu_{\text{C}=\text{O}}$ bands appear very similar between 1PE and 2PE, a clear difference is shown between 1PE and 2PE in the skeletal $\nu_{\text{C}=\text{C}}$ bands at 1450–1630 cm⁻¹ especially in the $\nu_{\text{C}=\text{C},\text{sym}}$ band.

Similarly, S_1 spectra of **II** in Figure 10B also show similarities and differences between 1PE and 2PE. Blue-shifted $\nu_{\text{C}=\text{C}}$ bands at 1550–1650 cm⁻¹ show very similar spectral shapes and overall bandwidths in both 1PE and 2PE except for the unresolved band around 1665 cm⁻¹ in 2PE. A group of red-shifted $\nu_{\text{C}=\text{C}}$ bands around 1420–1550 cm⁻¹ have similar frequencies in the 1PE and 2PE spectra, but the relative intensities for these $\nu_{\text{C}=\text{C}}$ bands are quite different. The symmetric $\nu_{\text{C}=\text{C}}$ band appearing at 1482–1490 cm⁻¹ gains significant absorption strength in the 2PE case with respect to the other $\nu_{\text{C}=\text{C}}$ bands.

Origin of the 1PE and 2PE S_1 Spectra. The recent literature on carotenoid photophysics has led to multiple suggestions of “new” electronic states in addition to the S_1 (2A_g^-) and S_2 (1B_u^+) states.^{48–51} Our data do not provide any evidence for an intermediate state (assumed to be the 1B_u^- state) lying between S_2 and S_1 , suggesting that it (a) lies above S_2 for these molecules, (b) has a lifetime of less than ~ 100 fs, or (c) has an infrared spectrum very similar to that of S_1 . Arguments for the involvement of the 1B_u^- state in the $S_2 \rightarrow S_1$ internal conversion are generally based on the energy gap law,²⁷ but for processes proceeding through conical intersections,^{18,19} the relevance of this argument is unclear.

Vibrational bands around 1500 cm⁻¹ have been assigned as $\nu_{\text{C}=\text{C},\text{sym}}$ of T_1 states for β -carotene and **I** in recent resonance Raman scattering studies.^{12,34,52} Thus, the long-lived infrared absorption bands including the very strong ones at 1510 and 1507 cm⁻¹ for **I** and **II**, respectively, with 2PE are very close to these frequencies, suggesting they may arise from the T_1 state. The $T_1 \rightarrow T_N$ absorption for **I** appears around 520 nm;^{53,54} however, visible transient absorption measurements between 500 and 550 nm for **I** with 2PE at 1275 nm did not show any absorption band with dynamics similar to that of the long-lived infrared absorption bands. Also the Raman spectrum of the T_1 state for **I** is quite similar to that of the ground state ($\nu_{\text{C}=\text{C},\text{sym}}$ has a 16 cm⁻¹ red shift and is broadened in the T_1 state),³⁴ which is quite different from what we saw in our infrared measurements. The strong absorption bands around 1510 cm⁻¹ are very much stronger than the vibrational bands of the singlet excited and ground states. We therefore exclude the triplet-state formation as the origin of the long-lived species with 2PE.

Another state, S^* , near S_1 has been proposed on the basis of ultrafast electronic spectroscopy, initially for spirilloxanthin ($N = 13$).⁴⁹ It is currently unsettled whether S^* is a hot ground state,^{50,55,56} a separate electronic state,^{49,57,58} or a conformational isomer of S_1 .^{51,59,60} In our experiments, the formation of a hot ground state is observed in the 1PE experiments of **II** in polar solvents (CHCl_3 , CD_3CN). A hot ground state is generated from the decay of the S_1 state, and it shows a ~ 12 and 8.2 ps decay in CHCl_3 and CD_3CN , respectively, which is the vibrational cooling time. The amplitudes of the hot-ground-state bands are strongly dependent on the relative values of the S_1 lifetime and the cooling time. Buckup et al. reported the existence of an S^* state as a hot ground state in β -carotene and its homologues.⁵⁵

The S* lifetimes for β -carotene and longer homologues are in the 7–10 ps range, while the S₁ lifetime varies from 9.5 to 1.0 ps. The exact lifetime of the S* state was not resolved in the case of a shorter β -carotene homologue where the S₁ lifetime is 42 ps. In this study, no intermediate state between the S₂ and S₁ states was observed for I and II. However, the formation of the hot ground state is seen for II in polar solvents where the S₁ lifetime is shorter than the vibrational cooling time (\sim 10 ps). Thus, the existence of a vibrationally hot ground state in the excited-state dynamics from the S₂ state of II in polar solvents might support the idea that S* is a hot ground state as proposed by Buckup et al.⁵⁵ However, experiments on longer carotenoids such as spirilloxanthin⁴⁹ are needed to unequivocally determine the nature of the S* state.

A particularly significant discussion for our purposes is that given by Fuss et al.¹⁸ These authors consider two coordinates for the discussion of the relative position of minima on the S₀, S₁, and S₂ potential surfaces—the bond alternation coordinate (δ) and the bond angle alternation coordinate (β). They suggest that the S₁ state surface has a double minimum along the angle alternation coordinate, while the ground state has a double minimum along δ . Although Fuss et al. suggest that for β -carotene two minima on S₁ are separated by a very small barrier, our data suggest that (a) the barrier is larger and that (b) internal conversion populates one minimum and direct 2PE to S₁ populates the other. Whether the two minima involve other coordinate changes such as a twist of the polyene backbone is not yet clear. Given that δ and β are proposed¹⁸ to be the principal coordinates spanning the conical intersection (between S₁ and S₀) branching space, it is not surprising that quite different dynamics are observed for the two minima within this scenario.

The relative equilibrium geometries of carotenoids, particularly along the bond alternation coordinate, do not seem to be fully settled. Kleinschmidt et al.⁶¹ found much reduced bond length alternation in S₂ compared to the ground state, whereas Dreuw⁶² in a study of *s-cis*-zeaxanthin found similar bond length alternation in S₀ and S₂ and significant flattening of the alternation in S₁. We hope that recent developments in electronic structure theory⁶³ will allow these structures to be determined unambiguously.

Concluding Remarks

The calculation of the electronic structure of carotenoids has long presented a major challenge to quantum chemistry.¹⁰ Despite recent impressive advances,^{61,63} a full exploration of the potential surface of the 2A_g⁻ state and the region of the conical intersection with the 1B_u⁺ state remains very challenging. We hope the results presented here showing the presence of two noncommunicating regions of S₁ with quite distinct infrared spectra will stimulate detailed investigation of the conformational space of these complex and fascinating molecules.

Acknowledgment. This research was funded by the NSF. We thank Prof. Lowell D. Kispert for his generous donation of 7',7'-dicyano-7'-apo- β -carotene and many thoughtful discussions concerning our findings.

References and Notes

- Niyogi, K. K. *Annu. Rev. Plant Physiol. Plant Mol. Biol.* **1999**, *50*, 333.
- Demmig-Adams, B.; Adams, W. W. *Science* **2002**, *298*, 2149.
- Frank, H. A.; Cogdell, R. J. *Photochem. Photobiol.* **1996**, *63*, 257.
- van Amerongen, H.; van Grondelle, R. *J. Phys. Chem. B* **2001**, *105*, 604.
- Ritz, T.; Damjanovic, A.; Schulten, K.; Zhang, J. P.; Koyama, Y. *Photosynth. Res.* **2000**, *66*, 125.
- von Lintig, J.; Hessel, S.; Isken, A.; Kiefer, C.; Lampert, J. M.; Voolstra, O.; Vogt, K. *Biochim. Biophys. Acta, Mol. Basis Dis.* **2005**, *1740*, 122.
- Sujak, A.; Gabrielska, J.; Grudzinski, W.; Borc, R.; Mazurek, P.; Gruszecki, W. I. *Arch. Biochem. Biophys.* **1999**, *371*, 301.
- Wang, X.-D.; Tang, G.-W.; Fox, J. G.; Krinsky, N. I.; Russell, R. M. *Arch. Biochem. Biophys.* **1991**, *285*, 8.
- BlanchardDesce, M.; Ledoux, I.; Lehn, J. M.; Malthete, J.; Zyss, J. *J. Chem. Soc., Chem. Commun.* **1988**, 737.
- Orlandi, G.; Zerbetto, F.; Zgierski, M. Z. *Chem. Rev.* **1991**, *91*, 867.
- Polívka, T.; Sundström, V. *Chem. Rev.* **2004**, *104*, 2021.
- Hashimoto, H.; Miki, Y.; Kuki, M.; Shimamura, T.; Utsumi, H.; Koyama, Y. *J. Am. Chem. Soc.* **1993**, *115*, 9216.
- Oneil, M. P.; Wasielewski, M. R.; Khaled, M. M.; Kispert, L. D. *J. Chem. Phys.* **1991**, *95*, 7212.
- He, Z. F.; Gosztola, D.; Deng, Y.; Gao, G. Q.; Wasielewski, M. R.; Kispert, L. D. *J. Phys. Chem. B* **2000**, *104*, 6668.
- He, Z. F.; Kispert, L. D.; Metzger, R. M.; Gosztola, D.; Wasielewski, M. R. *J. Phys. Chem. B* **2000**, *104*, 6302.
- Kopczynski, M.; Ehlers, F.; Lenzer, T.; Oum, K. *J. Phys. Chem. A* **2007**, *111*, 5370.
- Ehlers, F.; Wild, D. A.; Lenzer, T.; Oum, K. *J. Phys. Chem. A* **2007**, *111*, 2257.
- Fuss, W.; Haas, Y.; Zilberg, S. *Chem. Phys.* **2000**, *259*, 273.
- Garavelli, M.; Celani, P.; Bernardi, F.; Robb, M. A.; Olivucci, M. *J. Am. Chem. Soc.* **1997**, *119*, 11487.
- Mimuro, M.; Akimoto, S.; Takaichi, S.; Yamazaki, I. *J. Am. Chem. Soc.* **1997**, *119*, 1452.
- Bautista, J. A.; Connors, R. E.; Raju, B. B.; Hiller, R. G.; Sharples, F. P.; Gosztola, D.; Wasielewski, M. R.; Frank, H. A. *J. Phys. Chem. B* **1999**, *103*, 8751.
- Polívka, T.; Herek, J. L.; Zigmantas, D.; Åkerlund, H. E.; Sundström, V. *Proc. Natl. Acad. Sci. U.S.A.* **1999**, *96*, 4914.
- Walla, P. J.; Linden, P. A.; Hsu, C. P.; Scholes, G. D.; Fleming, G. R. *Proc. Natl. Acad. Sci. U.S.A.* **2000**, *97*, 10808.
- Zimmermann, J.; Linden, P. A.; Vaswani, H. M.; Hiller, R. G.; Fleming, G. R. *J. Phys. Chem. B* **2002**, *106*, 9418.
- Frank, H. A.; Bautista, J. A.; Josue, J. S.; Young, A. *J. Biochemistry* **2000**, *39*, 2831.
- Sashima, T.; Koyama, Y.; Yamada, T.; Hashimoto, H. *J. Phys. Chem. B* **2000**, *104*, 5011.
- Englman, R.; Jortner, J. *Mol. Phys.* **1970**, *18*, 145.
- Polívka, T.; Zigmantas, D.; Frank, H. A.; Bautista, J. A.; Herek, J. L.; Koyama, Y.; Fujii, R.; Sundstrom, V. *J. Phys. Chem. B* **2001**, *105*, 1072.
- Werncke, W.; Hogiu, S.; Pfeiffer, M.; Lau, A.; Kummrow, A. J. *Phys. Chem. A* **2000**, *104*, 4211.
- Christensen, R. L.; Goyette, M.; Gallagher, L.; Duncan, J.; DeCoster, B.; Lugtenburg, J.; Jansen, F. J.; van der Hoef, I. *J. Phys. Chem. A* **1999**, *103*, 2399.
- Frank, H. A.; Desamero, R. Z. B.; Chynwat, V.; Gebhard, R.; vanderHoef, I.; Jansen, F. J.; Lugtenburg, J.; Gosztola, D.; Wasielewski, M. R. *J. Phys. Chem. A* **1997**, *101*, 149.
- Hamm, P.; Kaindl, R. A.; Stenger, J. *Opt. Lett.* **2000**, *25*, 1798.
- Van Tassel, A. J.; Prantil, M. A.; Fleming, G. R. *J. Phys. Chem. B* **2006**, *110*, 18989.
- Hashimoto, H.; Koyama, Y. *Chem. Phys. Lett.* **1989**, *162*, 523.
- Jeevarajan, A. S.; Kispert, L. D.; Chumanov, G.; Zhou, C.; Cotton, T. M. *Chem. Phys. Lett.* **1996**, *259*, 515.
- Pang, Y.; Jones, G. A.; Prantil, M. A.; Fleming, G. R. Manuscript in preparation.
- Buckup, T.; Lebold, T.; Weigel, A.; Wohlleben, W.; Motzkus, M. *J. Photochem. Photobiol. A* **2006**, *180*, 314.
- Marder, S. R.; Torruellas, W. E.; BlanchardDesce, M.; Ricci, V.; Stegeman, G. I.; Gilmour, S.; Bredas, J. L.; Li, J.; Bublitz, G. U.; Boxer, S. G. *Science* **1997**, *276*, 1233.
- Krawczyk, S.; Olszowka, D. *Chem. Phys.* **2001**, *265*, 335.
- Noguchi, T.; Hayashi, H.; Tasumi, M.; Atkinson, G. H. *J. Phys. Chem.* **1991**, *95*, 3167.
- McCamant, D. W.; Kim, J. E.; Mathies, R. A. *J. Phys. Chem. A* **2002**, *106*, 6030.
- Yoshizawa, M.; Aoki, H.; Hashimoto, H. *Phys. Rev. B* **2001**, *63*, 180301.
- Kukura, P.; McCamant, D. W.; Mathies, R. A. *J. Phys. Chem. A* **2004**, *108*, 5921.
- Shim, S.; Mathies, R. A. *J. Phys. Chem. B* **2008**, *112*, 4826.
- Mikami, N.; Ito, M. *Chem. Phys.* **1977**, *23*, 141.
- Bray, R. G.; Hochstrasser, R. M.; Sung, H. N. *Chem. Phys. Lett.* **1975**, *33*, 1.

- (47) Wunsch, L.; Neusser, H. J.; Schlag, E. W. *Chem. Phys. Lett.* **1975**, *31*, 433.
- (48) Koyama, Y.; Rondonuwu, F. S.; Fujii, R.; Watanabe, Y. *Biopolymers* **2004**, *74*, 2.
- (49) Grdinaru, C. C.; Kennis, J. T. M.; Papagiannakis, E.; van Stokkum, I. H. M.; Cogdell, R. J.; Fleming, G. R.; Niederman, R. A.; van Grondelle, R. *Proc. Natl. Acad. Sci. U.S.A.* **2001**, *98*, 2364.
- (50) Wohleben, W.; Buckup, T.; Hashimoto, H.; Cogdell, R. J.; Herek, J. L.; Motzkus, M. *J. Phys. Chem. B* **2004**, *108*, 3320.
- (51) Cong, H.; Niedzwiedzki, D. M.; Gibson, G. N.; Frank, H. A. *J. Phys. Chem. B* **2008**, *112*, 3558.
- (52) Dallinger, R. F.; Farquharson, S.; Woodruff, W. H.; Rodgers, M. A. J. *J. Am. Chem. Soc.* **1981**, *103*, 7433.
- (53) Truscott, T. G.; Land, E. J.; Sykes, A. *Photochem. Photobiol.* **1973**, *17*, 43.
- (54) Becker, R. S.; Bensasson, R. V.; Lafferty, J.; Truscott, T. G.; Land, E. J. *J. Chem. Soc., Faraday Trans. 2* **1978**, *74*, 2246.
- (55) Buckup, T.; Savolainen, J.; Wohleben, W.; Herek, J. L.; Hashimoto, H.; Correia, R. R. B.; Motzkus, M. *J. Chem. Phys.* **2006**, *125*, 194505.
- (56) Savolainen, J.; Buckup, T.; Hauer, J.; Jafarpour, A.; Serrat, C.; Motzkus, M.; Herek, J. L. *Chem. Phys.* **2009**, *357*, 181.
- (57) Papagiannakis, E.; Kennis, J. T. M.; van Stokkum, I. H. M.; Cogdell, R. J.; van Grondelle, R. *Proc. Natl. Acad. Sci. U.S.A.* **2002**, *99*, 6017.
- (58) Papagiannakis, E.; Vengris, M.; Larsen, D. S.; van Stokkum, I. H. M.; Hiller, R. G.; van Grondelle, R. *J. Phys. Chem. B* **2006**, *110*, 512.
- (59) Niedzwiedzki, D. M.; Sullivan, J. O.; Polivka, T.; Birge, R. R.; Frank, H. A. *J. Phys. Chem. B* **2006**, *110*, 22872.
- (60) Niedzwiedzki, D.; Koscielcke, J. F.; Cong, H.; Sullivan, J. O.; Gibson, G. N.; Birge, R. R.; Frank, H. A. *J. Phys. Chem. B* **2007**, *111*, 5984.
- (61) Kleinschmidt, M.; Marian, C. M.; Waletzke, M.; Grimme, S. *J. Chem. Phys.* **2009**, *130*, 044708.
- (62) Dreuw, A. *J. Phys. Chem. A* **2006**, *110*, 4592.
- (63) Ghosh, D.; Hachmann, J.; Yanai, T.; Chan, G. K. L. *J. Chem. Phys.* **2008**, *128*, 144117.

JP905758E